Journal of Applied Electrochemistry **34**: 1013–1019, 2004.

Codeposition and microstructure of nickel–SiC composite coating electrodeposited from sulphamate bath

C.S. LIN[1]* and K.C. HUANG[2]
[1]*Department of Materials Science and Engineering, National Taiwan University Taipei 106, Taiwan*
[2]*Department of Mechanical Engineering, Da-Yeh University, Changhua 515, Taiwan*
*(*author for correspondence, fax: +886-2-23634562, e-mail: csclin@ntu.edu.tw)*

Received 8 December 2003; accepted in revised form 15 May 2004

Key words: adsorption isotherms, composite coating, electrodeposition, nickel sulphamate, thallium ions

Abstract

Ni–SiC composite coatings were electroplated from a nickel sulphamate solution with a SiC suspension, with and without the addition of monovalent thallium ions. Without thallium ions, the incorporated SiC particles did not modify the columnar grain structure of the nickel matrix. Conversely, the nickel matrix exhibited an equiaxed grain structure; meanwhile, the amount of codeposited SiC was markedly increased by adding thallium ions to the solution. Additionally, the density of lattice defects associated with nickel grains substantially decreased when the columnar grains were replaced by equiaxed grains. These distinct grain structures associated with the various coatings were discussed in terms of the inhibition of nickel electrocrystallization by thallium ions as well as the absorption and reduction of the various ionic species absorbed on the surface of the SiC particles.

1. Introduction

Electrodeposition of ceramic, polymer and metal powders within metal, ceramic or polymer matrix produces composite coatings with attractive properties such as wear-resistance, electrocatalysis and energy storage [1–4]. For applications of wear resistance and high-temperature strength, silicon carbide codeposited metal matrix composite coatings have been extensively studied with the aim of correlating the amount of codeposited particles to the bath composition and the concentration of suspended particles in the bath; the particle form, size and size distribution; the addition of surfactant and metallic ions; and the electroplating parameters such as temperature, pH, the type of imposed current, current density, and the type and degree of agitation [5–14]. In general, the amount of codeposited SiC in the composite coating increases with the concentration of suspended SiC [5–7, 14]. In a nickel sulphamate bath, the amount of codeposited SiC increases with DC current density [5], whereas a complex dependence of the amount of codeposited SiC was observed in a cobalt sulfate bath [6]. These distinct differences have led to the development of a modified mechanism based on Guglielmi's model [5]. The modified mechanism proposed by Hwang [6] incorporates the reduction of protons and cobalt ions on the surface of SiC particles to be a major step determining the amount of codeposited SiC with the cobalt matrix. The amount of codeposited SiC also depends strongly on the particle size. For submicron and micron sized SiC, Maurin and Lavanant [7] demonstrated that the amount of codeposited SiC increases as the particle size of SiC increases. Kim and Yoo [10] reported that a maximum codeposited amount in the sulphamate nickel bath is achieved for SiC of around 10 μm. Further increasing SiC size to 20 μm results in a decrease in the amount of codeposited SiC. Among the strategies for enhancing the amount of codeposited particles, the addition of organic additives [11, 12] and metal cations [14, 15] have been shown to effectively enhance the amount of codeposited particles, which is relatively insensitive to the bath composition and electroplating parameters. The addition of sodium hexanitrocobaltate or cationic surfactant containing an azobenzene group markedly promotes the codeposition of SiC in nickel coatings [11, 12]. Several monovalent cations, particularly the thallium ion, effectively promote the codeposition of nonconducting fine particles with electrodeposits of copper or nickel from acid baths [15–19]. This enhancement is considered to be associated with the modification of the surface charge of the particles by the absorbed molecules or ions, thereby promoting electrophoretic migration of the suspended particles. Additionally, the codeposition of the loosely adsorbed particles is further enhanced by the reduction of the absorbed ions [6, 16–20].

Although there is a wealth of literature concerning the effect of operating conditions on the amount of codeposited particles in the metal matrix and the resulting properties of composite coatings, the effect of

codeposited particles on the microstructure of composite coatings has only been investigated to a limited extent. Takahashi et al. [21] demonstrated that a Zn-22%Fe-7%SiO_2 electrodeposit exhibits a laminar structure consisting of bright and dark layers, as observed by transmission electron microscopy (TEM). SiO_2 particles, which are absent in dark layers, are preferentially codeposited in bright layers. Conversely, SiO_2 particles are uniformly distributed in a Zn-13%Cr-8%SiO_2 composite deposit, which displays a single layer structure as observed using cross-sectional TEM. For electroplating Ni–Al composite, Susan et al. [22] noted that the nucleation and growth of small nickel grains on the surface of Al particles refines the grain structure of the nickel matrix, particularly at high current density. In this study, we investigate how monovalent thallium ions in the solution affect the amount of codeposited SiC particles and modify the grain structure and lattice defects of nickel electrodeposits.

2. Experimental details

Nickel coatings were electroplated on copper plates from a 50 °C nickel sulphamate bath at current density of 4 A dm^{-2}. Prior to electroplating, the copper plates were polished with emery papers up to grade 2400, rinsed in distilled water, and finally activated in 5% sulfuric acid at room temperature. The nickel sulphamate solution contained 95 g l^{-1} nickel ions as nickel sulphamate, 40 g l^{-1} boric acid, 3 g l^{-1} nickel chloride, and 2 ml l^{-1} wetting agent (1 wt % sodium dodecyle sulfate). Solution pH was adjusted to 4 using sulphamate acid or dilute sodium hydroxide solution. To make Ni–SiC composite coatings, 20 g l^{-1} SiC powder (Alfa, Johnson Matthey, α-SiC of 99.8% purity) with an average size of 2 μm was added to the nickel sulphamate solution. In addition, 0.5 g l^{-1} monovalent thallium ions as thallium sulfate were added to promote the codeposition of SiC particles. The three different deposits studied were designated as: sample A plated from the nickel sulphamate solution, sample B from the solution with the addition of 20 g l^{-1} SiC particles, and sample C from the solution with the addition of 20 g l^{-1} SiC particles and 0.5 g l^{-1} thallium ions. Electroplating was performed using a flow cell in which SiC particles were dispersed and circulated by pumping the solution to the plating cell consisting of a vertical anode and cathode separated by a distance of 30 mm. Electroplating was carried out for 85 min, and the thickness of the resulting deposits was approximately 70 μm.

The structure of various deposits was first observed using conventional cross-sectional metallography specimens. The volume percent of codeposited SiC was measured via LECO 2001 image analysis system. A combined mechanical grinding and ion-beam thinning technique was used to prepare cross-sectional TEM specimens [23, 24]. The defect structure of the nickel matrix was characterized using selected-area diffraction (SAD) and nano-beam diffraction (NBD) techniques. Phase identification and preferred orientation of various coatings were carried out using X-ray diffraction (XRD) with a copper target operating at 40 kV and 30 mA. Finally, the hardness of the distinct deposits was measured on the polished cross sections with an applied load of 50 g. The hardness of each deposit was reported as an average of five measurements.

3. Results

3.1. *Deposit microstructure*

Figure 1 shows the morphology, shape and size distribution of the SiC particles used for preparing the composite coating. Relatively large SiC particles were platelets with sizes ranging from 1 to 3 μm. Relatively small SiC particles were equi-axial and tended to agglomerate onto the flat surfaces of relatively large SiC platelets, as indicated by the arrow in Figure 1.

Figure 2 illustrates the cross sections of the various deposits observed under an optical microscope. Samples A and B exhibited a columnar structure, which is a characteristic of the nickel coatings plated from the nickel sulphamate bath without organic additives [24, 25]. The volume percentage of SiC particles codeposited in sample B was estimated to be 6.1%. SiC particles in the solution did not affect the grain structure of nickel deposits as only 6% of SiC particles were incorporated into the coating, suggesting that SiC particles in the solution barely affected the electrocrystallizaition of nickel. Figure 2(c) shows the addition of 0.5 g l^{-1} thallium ions led to the codeposition of about 17.1% SiC particles. This modest amount of codeposited SiC particles or the presence of thallium ions in the solution notably modified the microstructure of the nickel matrix, which was too fine to be resolved using a conventional chemical etching method [24].

Figure 3 shows the cross-sectional TEM micrograph, illustrating that the nickel coating plated from a nickel

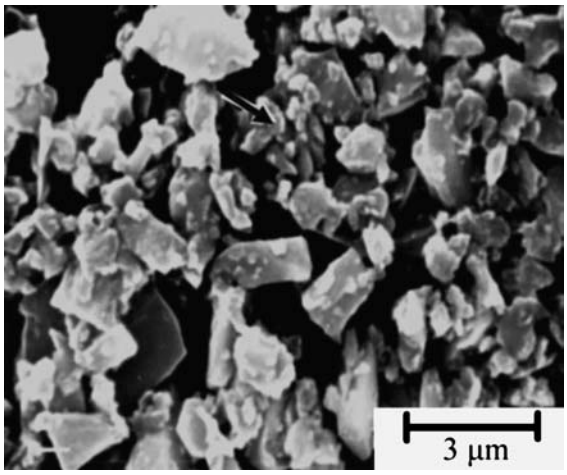

Fig. 1. SEM micrograph showing the morphology, shape and size distribution of the SiC particles.

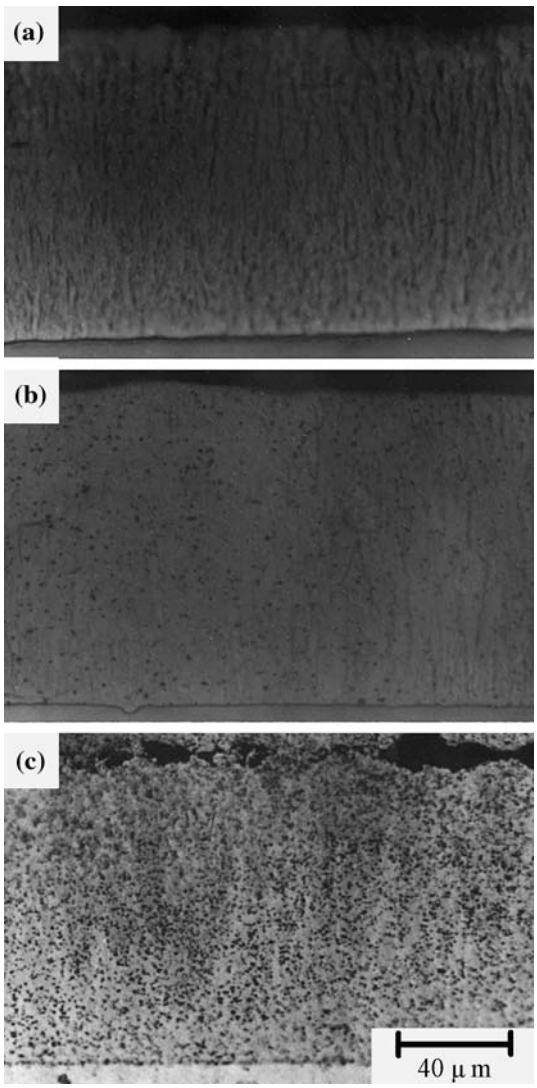

Fig. 2. Cross-sectional optical micrographs of the distinct coatings: (a) pure nickel, (b) Ni–SiC composite coating plated from the bath without the addition of thallium ions, and (c) Ni–SiC composite coating plated from the bath with 0.5 g l^{-1} thallium ions.

sulphamate solution displayed a columnar grain structure. These columnar grains contained a high density of dislocations and twins where the twin planes notably remained parallel to the columnar axis of the nickel grains. The width of the columnar grains must be determined since the twin planes remain parallel to the columnar axis of each columnar grain [24]. The population density of twins has been shown to markedly affect the recrystallization behaviour of the nickel deposits [25]. Moreover, the nickel deposits of distinct textures may have different twin plane organizations [26].

Cross-sectional TEM also revealed that sample B had a columnar grain structure with a high density of lattice defects such as twins and dislocations. SiC particles, which were identified using EDS, exhibited a uniform and light diffraction contrast when observed along most of the orientations relative to incident electron beams, as indicated by the arrows in Figure 4(a) and (b). Moreover, SiC particles generally had sharp and flat edges,

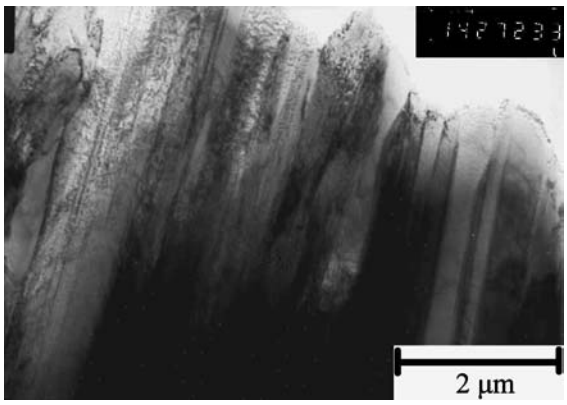

Fig. 3. Cross-sectional TEM micrograph of sample A illustrating columnar nickel grains.

which are consistent with the platelet morphology observed via SEM (Figure 1). The large flat face of each platelet oriented randomly to columnar nickel grains; that is, some SiC particles (marked by the arrow in Figure 4(b)) had their large flat faces parallel to the columnar axis, while some of them were perpendicular to the columnar axis (marked by the arrows in Figure 4 (a)). The random orientations of codeposited SiC particles relative to columnar nickel grains suggest a random adsorption of SiC particles onto nickel. In contrast, for electroplating Ni–SiC composite coatings on a rotating disc electrode, Maurin and Lavanant [7] illustrated that the emerging SiC platelets are not fixed to the nickel along their large flat cleavage faces but stand vertically. Figure 5 shows a codeposited SiC

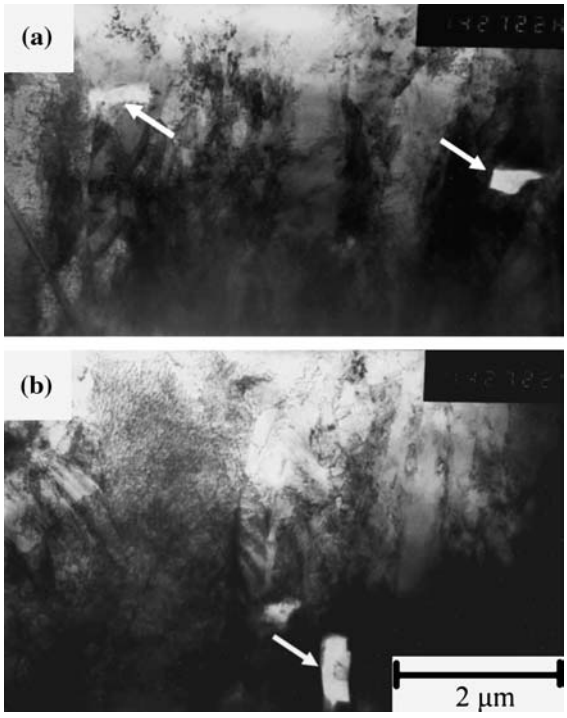

Fig. 4. (a) Cross-sectional TEM micorgraphs of sample B showing the large flat face of the SiC particles is perpendicular to columnar nickel grains, or (b) parallel to the long axis of the columnar nickel grains.

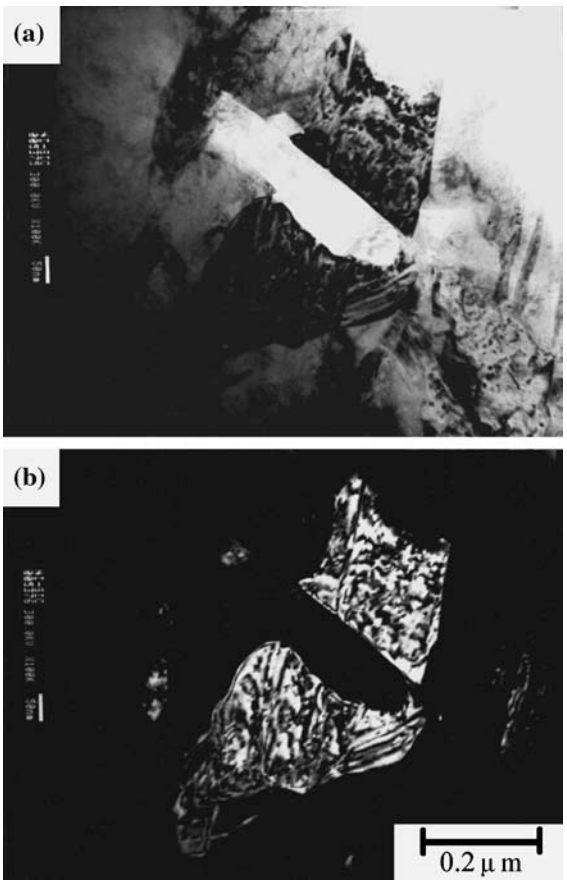

Fig. 5. Cross-sectional TEM micrographs of sample B: (a) bright field and (b) dark field images.

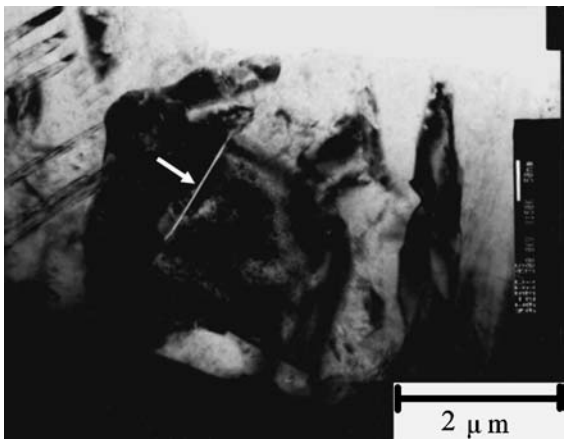

Fig. 6. Cross-sectional TEM micrograph of sample B showing cracks at the interface between SiC platelet and the nickel matrix.

platelet, with a large flat face perpendicular to and across two columnar nickel grains. The dark field image (Figure 5(b)), shows that codeposited SiC particle had little effect on the development of columnar grains since the growth of columnar grains continued across the SiC platelet codeposited at the moving interface between nickel grains and the solution. Moreover, cracks were frequently observed at one of the boundaries between SiC particles and the nickel matrix (as shown by the arrow in Figure 6) when observed at certain edge-on conditions.

A significant increase in the volume percentage of codeposited SiC was observed once thallium ions were added to the solution. Figure 7(a) shows that the nickel deposits displayed an equiaxed grain structure. Again, codeposited SiC particles exhibited a light contrast, as indicated by the arrows. Furthermore, the nickel coating displayed a bimodal grain structure, namely, relatively large nickel grains were dotted with fine nickel grains (Figure 7(b)). The average size of the relatively large grains was about 1 μm, whereas the typical size of fine grains (the arrows) was less than 0.1 μm. EDS spectra taken from fine grains contained nickel signals only. The thallium signal was below the detectable limit of EDS, which was about 1 wt %. NBD patterns show that these fine grains were FCC nickel, as illustrated by the patterns along F.C.C. (111) and (110) zone axes shown in Figure 7(d) and (e), respectively. The nickel grains also contained dislocations and twins which were readily identified on the dark-field image (the arrow in Figure 7(c)) and the (110) pattern (Figure 7(e)). The density of twins associated with sample C was apparently less than that associated with samples A or B.

Figure 8 shows the XRD patterns of samples A and C, as well as the coating made from the nickel sulphamate solution in the presence of 0.5 g l^{-1} thallium ions. Figure 8(a) shows that the pure nickel coating, which contained vertical twin planes (Figure 3), had a (110) texture. Amblard et al. [26] prepared nickel coatings from a Watts bath and noted that the coating with vertical twin planes (the planes parallel to columnar axis) exhibited a (211) texture. On the other hand, the nickel coating plated from a sulphamate bath at 50 °C had a (110) texture and contained a high density of dislocations and twins with twin planes parallel to the columnar axis [24]. Consequently, the anions in the solution affect, to some extent, the texture and twin plane organizations of the nickel deposits. Twins have been further identified as being associated with the crystal symmetry of nickel coatings plated from a Watts bath [27, 28]. For example, the deposits of (110) texture obtained at a high cathodic potential have a fivefold symmetry, and the nickel grains are made up of five identical areas separated by twins. Meanwhile, those of (211) texture exhibit a twofold symmetry and the nickel grains are divided into two parts by groups of twins of uneven number.

The addition of SiC particles to the solution did not modify the texture of the nickel coating since the composite coating (sample B) also displayed a (110) texture. In contrast, the composite coating (sample C) plated from the nickel sulphamate solution containing SiC particles and thallium ions showed a random orientation (Figure 8(b)). To investigate the effect of thallium ions on the electrocrystallization of nickel, a coating was plated from the nickel sulphamate solution with the addition of 0.5 g l^{-1} thallium ions. Like sample C, this coating displayed a random orientation, as can

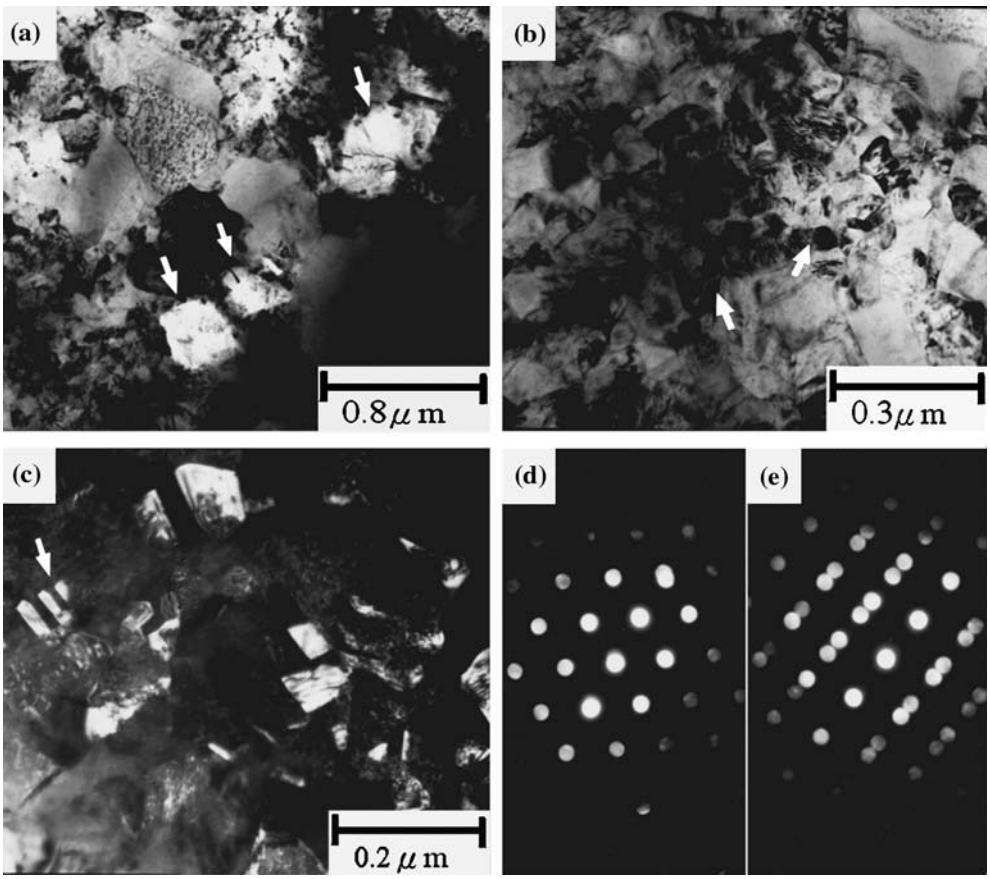

Fig. 7. (a)–(c) Cross-sectional TEM micrographs of sample C, and (d) and (e) the nano-beam electron diffraction patters from an equiaxed nickel grain.

be seen in Figure 8(c). Moreover, the diffraction peaks corresponding to metallic thallium were also noted. This random orientation correlates well with the equiaxed grains observed using cross-sectional TEM (Figure 9(a)). Furthermore, the presence of thallium signals on the EDS spectrum (Figure 9(b)) is also consistent with the peaks of thallium observed on the XRD pattern.

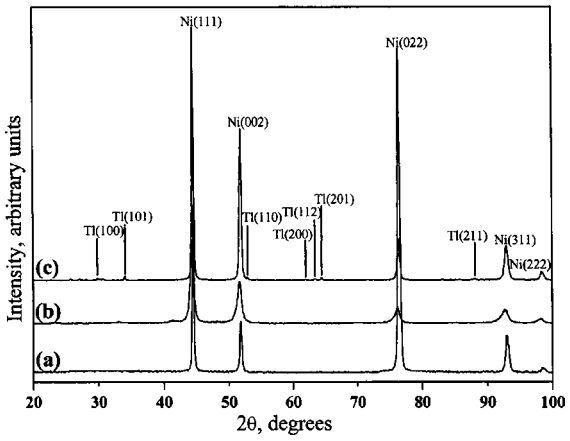

Fig. 8. XRD patterns of the distinct coatings: (a) sample A, (b) sample C, and (c) the coating plated from the nickel sulphamate bath with the addition of 0.5 g l^{-1} thallium ions.

3.2. *Deposit hardness*

The hardness of the various deposits was 296.0 ± 8.0, 320.0 ± 8.5, and 523.0 ± 20.0 kg mm^{-2} for samples A, B, and C, respectively. Although codeposited SiC particles may lead to an increase in the hardness of the deposits, the refinement in the nickel grains by thallium ions in the solution and by codeposited SiC particles also account for the enhancement of the strength of the deposits.

4. Discussion

During the codeposition of inert particles and metal matrix, it is generally recognized that the inert particles are first transported toward the cathode hydrodynamically [20, 29]. Such transportation is further enhanced when certain ionic species are adsorbed on the inert particles; particularly the positive ionic cloud surrounding the particles. Reduction of the adsorbed ionic species also causes the incorporation of inert particles in the metal matrix [5, 6, 16–20]. In a nickel sulphamate solution, both protons and nickel ions are potentially adsorbed on SiC particles. Reduction of absorbed nickel ions provides a bonding between SiC particles and nickel grains, leading to strong adsorption and

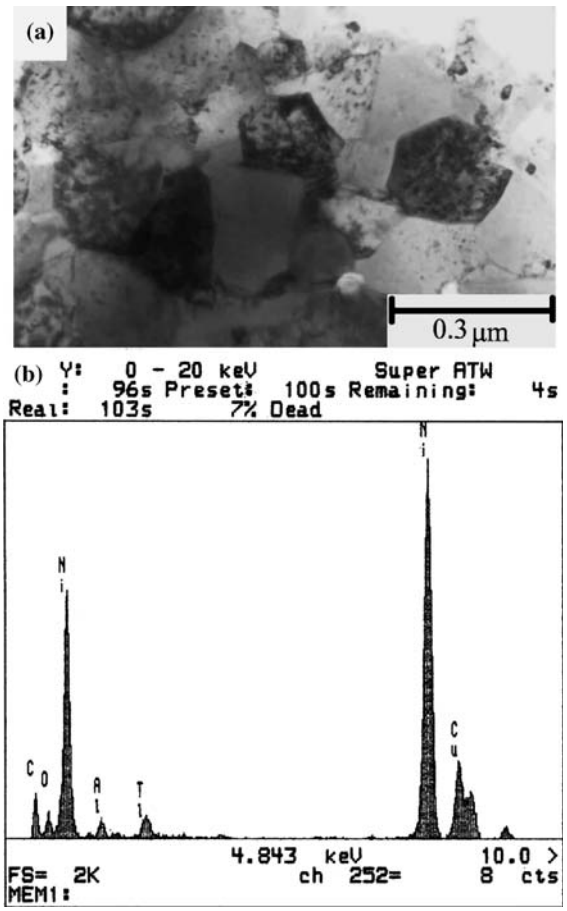

Fig. 9. (a) TEM micrograph and (b) EDS spectrum of the coating plated from the nickel sulphamate bath with the addition of 0.5 g l^{-1} thallium ions.

then incorporation of SiC particles on nickel. Conversely, protons absorbed on SiC particles cause a screen effect on prohibiting the direct reduction of nickel ions on SiC particles. Microcracks along the interface between SiC particles and the nickel matrix deposited from the solution without thallium ions can thus be ascribed to protons absorbed on SiC particles. Because codeposited SiC particles randomly intersect columnar nickel grains whose orientations remain unchanged across each SiC particle, incorporated SiC particles apparently do not provide additional nucleation sites for the electrocrystallization of nickel. This result suggests that the reduction of nickel ions on SiC particles is limited due to the absorption of protons on the particles. When electroplating the composite coatings with alumina particles in a nickel or copper matrix, White and Foster [19] demonstrated that poor adhesion of alumina particles to metal matrix prevails at lower pH as the weight of the nickel ions absorbed on alumina decreases with decreasing pH. In an acidified copper sulfate solution, Roos et al. [18] noted that the adsorption of protons onto the alumina surface impedes the adsorption of other cations, such as copper and aluminium ions, thereby hindering the codeposition of alumina.

Once thallium ions are added to a nickel sulphamate bath, they may compete with protons and nickel ions to be absorbed on SiC particles. Reduction of absorbed thallium ions, if they happen to be the major ionic species adsorbed, can provide a bonding between inert particles and the nickel matrix, or even serves as potential nucleation sites for the electrocrystallization of nickel. Both EDS and XRD measurements reveal that together with the electrocrystallization of nickel, thallium is electroplated from the nickel sulphamate solution containing 0.5 g l^{-1} thallium ions. Furthermore, when both SiC particles and thallium ions are added to a nickel sulphamate solution, thallium peaks are absent on the XRD pattern. This dramatic decrease in the amount of thallium in the deposit indicates that thallium ions have been absorbed on SiC particles, allowing less free thallium ions in the solution to participate in the electrocrystallization of nickel. The thallium ions absorbed on SiC particles can thus contribute to an increase in the amount of codeposited SiC particles, although other mechanisms may also play an important role in enhancing the codeposition of SiC particles. For example, thallium ions may modify the adsorption isotherms of nickel ions and protons [16] to favor the adsorption of nickel ions, or act as a catalyst [17, 18] for the reduction of nickel ions absorbed on SiC particles. Then, nickel ions become the major ionic species reduced on SiC particles, allowing for bonding between the nickel matrix and SiC particles as well as promoting the nucleation of nickel grains. Furthermore, adding thallium ions to the nickel sulphamate solution containing SiC particles leads to the formation of equiaxed grains since thallium ions absorbed on nickel strongly inhibit the growth of nickel grains.

5. Conclusions

The effect of codeposited SiC particles on the microstructure of the nickel matrix was investigated, with emphasis on the addition of monovalent thallium ions. The cross section of the nickel coating plated from a nickel sulphamate solution exhibited a characteristic columnar structure containing numerous dislocations and twins. Without the addition of thallium ions, codeposited SiC particles did not alter the grain structure and texture of the nickel matrix although approximately 6% (in volume) of SiC particles were incorporated in the nickel matrix. Furthermore, cracks were frequently observed on the interface between the nickel matrix and SiC particles. Adding 0.5 g l^{-1} thallium ions to the solution with a SiC suspension substantially enhanced the codeposition of SiC particles and led to the formation of equiaxed nickel grains. However, thallium signals and diffraction peaks were absent respectively from the EDS spectrum and XRD pattern taken from this composite coating, indicating that thallium, if codeposited in the deposit, was below the detectable limit. Conversely, thallium was electro-

plated with nickel from the nickel sulphamate solution containing 0.5 g l^{-1} thallium ions. SiC particles in the solution apparently reduced the amount of thallium in the coating, suggesting that thallium ions were indeed absorbed on the SiC particles, which, in turn, promoted the codeposition of SiC particles in the deposit.

Unlike coarse columnar nickel grains plated from the nickel sulphamate bath, the coating consisted of fine equiaxed grains when thallium ions were added to the solution. This grain refinement effect was due to the presence of thallium ions that, if absorbed onto nickel, inhibited the growth of nickel grains. Furthermore, thallium ions absorbed on SiC particles might modify the adsorption isotherms of nickel ions and protons or act as a catalyst for the reduction of nickel ions. The reduction of nickel ions on SiC particles provided additional nucleation sites for the electrocrystallization of equiaxed nickel grains.

Columnar nickel coatings plated from a sulphamate nickel bath generally contained vertical twin planes and exhibited a (110) texture. Conversely, equiaxed nickel grains plated from the solution with thallium ions had a random orientation. The defect density associated with nickel grains was reduced once columnar grains were modified to equiaxed grains.

Acknowledgements

This research was supported by the National Science Council, Republic of China, under grant No. 902216E212001. The authors wish to thank Ms L. C. Wang for her assistance with the TEM work, and Dr L. Cheng of China Steel Corporation for his invaluable discussion. This study made use of the Electron Microscopes of National Sun Yet-sen University and National Chung Hsing University, supported by the National Science Council, Republic of China.

References

1. J. Fransaer, J.P. Celis and J.R. Roos, *Metal Finish.* **91** (June 1993) 97.
2. K. Helle and F. Walsh, *Trans. IMF* **75** (1997) 53.
3. M. Musiani, *Electrochim. Acta* **45** (2000) 3397.
4. A.C. Tavares and S. Trasatti, *Electrochim. Acta* **45** (2000) 4195.
5. N. Guglielmi, *J. Electrochem. Soc.* **119** (1972) 1009.
6. B.J. Hwang and C.S. Hwang, *J. Electrochem. Soc.* **140** (1993) 979.
7. G. Maurin and A. Lavanant, *J. Appl. Electrochem.* **25** (1995) 1113.
8. O. Berkh, S. Eskin and J. Zahavi, *Plat. Surf. Finish.* **81** (March 1994) 62.
9. L. Orlovskaja, N. Periene, M. Kurtinaitiene and S. Surviliene, *Surf. Coat. Technol.* **111** (1999) 234.
10. S.K. Kim and H.J. Yoo, *Surf. Coat. Technol.* **108–109** (1998) 564.
11. N.K. Shrestha, I. Miwa and T. Saji, *J. Electrochem. Soc.* **148** (2001) C106.
12. L. Benea, P.L. Bonora, A. Borello, S. Martelli, F. Wenger, P. Ponthiaux and J. Galland, *J. Electrochem. Soc.* **148** (2001) C461.
13. A.F. Zimmerman, D.G. Clark, K.T. Aust and U. Erb, *Mater. Lett.* **52** (2002) 85.
14. S.C. Wang and W.C. Wei, *Mater. Chem. Phys.* **78** (2003) 574.
15. T.W. Tomaszewski, L.C. Tomaszewski and H. Brown, *Plating* **56** (1969) 1234.
16. K.M. Yin and H.J. Hong, *Trans. IMF* **75** (1997) 35.
17. J.P. Celis and J.R. Roos, *J. Electrochem. Soc.* **124** (1977) 1508.
18. J.R. Roos, J.P. Celis and J.A. Helsen, *Trans. IMF* **55** (1977) 113.
19. C. White and J. Foster, *Trans. IMF* **56** (1978) 92.
20. M.J. Bhagwat, J.P. Celis and J.R. Roos, *Trans. IMF* **61** (1983) 72.
21. A. Takahashi, Y. Miyoshi and T. Hada, *J. Electrochem. Soc.* **141** (1994) 954.
22. D.F. Susan, K. Barmak and A.R. Marder, *Thin Solid Films* **307** (1997) 133.
23. C.S. Lin, H.B. Lee and S.H. Hsueh, *Metall. Mater. Trans. A* **30** (1999) 437.
24. C.S. Lin, K.C. Peng, P.C. Hsu, L. Chang and C.H. Chen, *Mater. Trans. JIM* **41** (2000) 777.
25. C.S. Lin, P.C. Hsu, K.C. Peng, L. Chang and C.H. Chen, *Mater. Trans. JIM* **42** (2001) 316.
26. J. Amblard, M. Froment, G. Maurin and N. Spyrellis, *J. Microsc. Spectrosc. Electron.* **6** (1981) 311.
27. I. Epelboin, M. Froment and G. Maurin, *Plating* **56** (1969) 1356.
28. J. Amblard, I. Epelboin, M. Froment and G. Maurin, *J. Appl. Electrochem.* **9** (1979) 233.
29. J. Fransaer, J.P. Celis and J.R. Roos, *J. Electrochem. Soc.* **139** (1992) 413.